Research Article

Journal of Applied Toxicology

Received: 20 January 2013, Revised: 13 April 2013, Accepted: 21 April 2013 Published online in Wiley Online Library: 22 July 2013

(wileyonlinelibrary.com) DOI 10.1002/jat.2900

Oxidative stress increased hepatotoxicity induced by nano-titanium dioxide in BRL-3A cells and Sprague–Dawley rats

Baoyong Sha[a,b,c], Wei Gao[d], Shuqi Wang[e], Xingchun Gou[a], Wei Li[f], Xuan Liang[g], Zhiguo Qu[h], Feng Xu[b,c]* and Tian Jian Lu[c]*

ABSTRACT: Extensive studies have shown that titanium dioxide (TiO_2) nanomaterials (NMs) can cause toxicity *in vitro* and *in vivo* under normal conditions. However, an adverse effect induced by nano-TiO_2 in many diseased conditions, typically characterized by oxidative stress (OS), remains unknown. We investigated the toxicity of nano-TiO_2 in rat liver cells (BRL-3A) and Sprague–Dawley (SD) rat livers under OS conditions, which were generated using hydrogen peroxide (H_2O_2) *in vitro* and alloxan *in vivo*, respectively. *In vitro* results showed that cell death ratios after nano-TiO_2 exposure were significantly enhanced (up to 2.62-fold) in BRL-3A cells under OS conditions, compared with normal controls. Significant interactions between OS conditions and nano-TiO_2 resulted in the rapid G0/G1 to S phase transition and G2/M arrest, which were opposite to G0/G1 phase arrest in cells after NMs exposure only. *In vivo* results showed that obvious pathological changes in rat livers and the increased activities of four enzymes (i.e. aspartate aminotransferase, alanine aminotransferase, lactate dehydrogenase and alkaline phosphatase) owing to liver damage after nano-TiO_2 exposure under OS conditions, compared with their healthy controls. In addition, compared with increased hepatotoxicity after nano-TiO_2 exposure, micro-TiO_2 showed no adverse effects to cells and rat livers under OS conditions. Our results suggested that OS conditions synergistically increase nano-TiO_2 induced toxicity *in vitro* and *in vivo*, indicating that the evaluation of nanotoxicity under OS conditions is essentially needed prior to various applications of NMs in foods, cosmetics and potential treatment of diseases. Copyright © 2013 John Wiley & Sons, Ltd.

Supporting information can be found in the online version of this article.

Keywords: nano-titanium dioxide; hydrogen peroxide; alloxan; nanotoxicity; cell; rat

Introduction

Titanium dioxide (TiO_2) nanomaterials (NMs) have been widely used in foods, sunscreens, sports clothes, surface cleaning agents, automobile coatings and computer devices, because of their unique physicochemical properties such as heterogeneous and photocatalytic catalysis (Chen and Mao, 2007; Kocbek *et al*., 2010; Magrez *et al*., 2009; Sha *et al*., 2013a; Veronesi *et al*., 2012). However, the use of nano-TiO_2 has raised concerns owing to the increasing reports on their adverse effects in cell lines and animal models. For example, nano-TiO_2 can lead to cellular dysfunction, mRNA overexpression, oxidative damage and apoptosis in rat and human cells (sha *et al*., 2013b; Jugan *et al*., 2012; Kocbek *et al*., 2010; Qu *et al*., 2013). In addition, nano-TiO_2 can impair the spatial recognition memory, affecting biological functions of the knee joint and liver tissues in rodents (Fabian *et al*., 2008; Hu *et al*., 2010; Umbreit *et al*., 2012; Wang *et al*., 2009a). Although a great deal of effort has been made to reduce the toxicity of nano-TiO_2 (e.g. surface modification) (Warheit *et al*. 2005), stringent evaluations of nanotoxicity are still needed for their wide applications in daily life.

Nowadays, the adverse effects of nano-TiO_2 have been primarily assessed under normal conditions where healthy cells and experimental animals are exposed to TiO_2 NMs. However, as the mainstream NMs, the adverse effects of nano-TiO_2 under diseased status, especially oxidative stress (OS), have not been fully understood (Vicent and Duncan, 2006). OS is generally

* Correspondence to: Feng Xu, MOE Key Laboratory of Biomedical Information Engineering, School of Life Science and Technology, Xi'an Jiaotong University, Xi'an 710049, People's Republic of China. E-mail: fengxu@mail.xjtu.edu.cn

Tian Jian Lu, Bioinspired Engineering and Biomechanics Center, Xi'an Jiaotong University, Xi'an 710049, People's Republic of China. E-mail: tjlu@mail.xjtu.edu.cn

[a]Lab of Cell Biology & Translational Medicine, Xi'an Medical University, Xi'an, 710021, People's Republic of China

[b]MOE Key Laboratory of Biomedical Information Engineering, School of Life Science and Technology, Xi'an Jiaotong University, Xi'an, 710049, People's Republic of China

[c]Bioinspired Engineering and Biomechanics Center, Xi'an Jiaotong University, Xi'an, 710049, People's Republic of China

[d]Department of Anesthesiology, the First Affiliated Hospital of Medical College, Xi'an Jiaotong University, Xi'an, 710061, People's Republic of China

[e]Brigham and Women's Hospital, Harvard Medical School, Boston, MA, USA

[f]Graduate School of the Fourth Military Medical University, Xi'an, 710032, People's Republic of China

[g]Department of Stomatology, Second Provincial People's Hospital of Gansu, Lanzhou, 730000, People's Republic of China

[h]School of Thermal Energy and Power Engineering, Xi'an Jiaotong University, Xi'an, 710049, People's Republic of China

caused by the imbalance between oxidants and antioxidants, which represents the conditions of cells, tissues, organs, playing important roles in disease progression of fatty liver disease, type 2 diabetes, Parkinson's disease and heart failure (Codoner-Franch *et al*., 2010; Desai *et al*., 2010; Dut *et al*., 2008; Hoek and Pastorino, 2002; Jenner, 2003; Mantena *et al*., 2008; Nojiri *et al*., 2006; Van Gaal *et al*., 2006). In previous reports, it was found that the OS conditions of human bronchial epithelial cells can increase the cytotoxicity of ZnO NMs *in vitro* (Heng *et al*., 2010). Thus, it would be essential to understand the mutual effects between TiO_2 nanotoxicity and OS conditions *in vitro* and *in vivo* so as to guide the use of nano-TiO_2 in diseased conditions.

Kupffer cells and macrophages in the liver can clear the circulating NMs from various exposure routes [e.g. ingestion, breath, skin, intravenous (i.v.) and intraperitoneal (i.p.) injection] and accumulate them in liver tissues (Asakura *et al*., 2010; Sadauskas *et al*., 2009). For example, after injection of 5 mg kg^{-1} nano-TiO_2 to Male Wistar rats for 24 h, the liver is the dominant organ where NMs accumulate in normal conditions (Fabian *et al*., 2008). For i.p. injection of nano-TiO_2, the highest distribution of nano-TiO_2 was exhibited in ICR mice liver after short-term NMs exposure (Liu *et al*., 2009). As a result of the obvious accumulation of NMs in the liver, we focus on the NMs-induced hepatotoxicity under OS conditions.

In this study, we used hydrogen peroxide (H_2O_2) and alloxan to induce artificial OS conditions in liver cell (BRL-3A cell line) and Sprague–Dawley (SD) rat liver, separately. Then, the responses of cells and rats were tested after nanoscale and microscale TiO_2 exposure. Compared with the normal cell control, we observed that nano-TiO_2 significantly decreased cell viability and led to an aberrant cell cycle in BRL-3A cells under OS conditions. We also observed that OS conditions enlarged rat hepatic damage after nano-TiO_2 exposure. However, micro-TiO_2 showed no significant *in vitro* and *in vivo* effect under OS conditions. This study suggested that nano-TiO_2 and OS conditions reacted synergistically and significantly enhanced the hepatotoxicity *in vitro* and *in vivo*, highlighting the importance to understand the NMs-induced toxicity in diseased status for biomedical applications.

Materials and Methods

Reagent preparation

All reagents and chemicals were supplied by Sigma-Aldrich Trading Co. Ltd (Shanghai, China). Fetal calf serum (FBS) and cell culture media were obtained from Thermo Fisher Scientific (Beijing, China). Glutathione (GSH), aspartate aminotransferase (AST), alanine aminotransferase (ALT), lactate dehydrogenase (LDH) and alkaline phosphatase (ALP) enzyme linked immunosorbent assay (ELISA) kits were purchased from Roche Ltd. (Shanghai, China) and Jiancheng Bioengineering Company (Nanjing, China).

Characterization of TiO_2

Microscale TiO_2 powder (rutile phase, 1–5 μm in diameter and ≥ 99.9% trace metals basis) was obtained from Sigma-Aldrich Co. Ltd. For nano-TiO_2, the morphology and structure were measured using high-resolution transmission electron microscopy (HRTEM, JEOL JEM-2100 F), scanning electron microscope (SEM, JSM-6700 F) and X-ray diffraction (XRD, XRD-7000 s), respectively. Dynamic light scattering (DLS) was used to obtain the zeta potential and size distribution of nano-TiO_2 (Zetasizer Nano ZS90) (Asakura *et al*., 2010). The surface area of nano-TiO_2 was performed via the Brunauer–Emmett–Teller method (Micromeritics ASAP 2020® Accelerated Surface Area and Porosimetry analyzer) (Ribeiro *et al*., 2007).

Cell culture

The BRL-3A cell line was supplied by the Cell Bank of Type Culture Collection of Chinese Academy of Sciences (Shanghai, China). The BRL-3A cell was cultured in RPMI 1640 with 10% (v/v) FBS at 37 °C with 5% CO_2 using a cell incubator (Thermo Forma 371; Thermo Fisher Scientific). After the dissociation of adherent cells with Trypsin- ethylenedinitriletetraacetic acid (EDTA) (0.25%), cells was counted using a hemocytometer and transferred to new culture flasks for cell subculture. The cell density was fixed at 300 cells per mm^2 and all cells were incubated in 96-well culture plates throughout the cell experiments (Taurog *et al*. 1952).

MTT assay

The MTT [3-(4,5-Dimethylthiazol-2-yl)-2,5-diphenyltetrazolium bromide] method was used to test cell viability after H_2O_2 and/or TiO_2 exposure (Taurog *et al*., 1952). The difference between optical density (OD) values of formazan at 570 and 630 nm was collected to avoid the potential interference of physicochemical properties of TiO_2 (Ghosh *et al*., 2010; Sha *et al*., 2011). Each experimental concentration has six independent replicates for the statistical analysis.

H_2O_2 induced OS conditions in BRL-3A cells

BRL-3A cells were incubated with different concentrations of H_2O_2 (0.01, 0.1, 1, 10, 100 μM, 1, 10, 100 mM, 1 and 10 M) for 1, 6, 12 and 24 h to induce OS conditions. During exposure periods, we kept the cell incubator as a dark room. The intracellular OS endpoints were determined in no light environment immediately after H_2O_2 exposure. The generation of superoxide anion (O_2^-) in the BRL-3A cell was measured using the conversion of dihydroethidium to ethidium bromide (Bautista *et al*., 1990). Cellular lipid peroxidation was assessed by determining the level of malondialdehyde (MDA) according to the protocol reported in the literature (Buege and Aust, 1978). For antioxidant enzyme, the level of superoxide dismutase (SOD) was monitored through its ability to inhibit the photochemical reduction of nitroblue tetrazolium to blue formazan (Kuo *et al*., 2011). The change in the GSH level was determined using the ELISA kit, because GSH can react with 5, 50-dithiobis (2-nitrobenzoic acid) (DTNB) and lead to the generation of glutathione disulfide (GSSG) and 2-nitro-5-thiobenzoic acid (Wang *et al*., 2009b). Finally, three concentrations of H_2O_2 (1, 10 and 100 μM) and 1-h incubation time were chosen to induce the OS conditions before cell–TiO_2 interactions.

Toxicity assessment in BRL-3A cells

For cell experiments, TiO_2 suspensions were prepared in phosphate-buffered saline (PBS) according to previous literature (Chen *et al*., 2006; Sha *et al*., 2011). After 30 min of ultrasonication, four different concentrations (0.1, 1, 10 and 100 μg ml^{-1}) of nanoscale or microscale TiO_2 suspensions were added to cells

Journal of Applied Toxicology

immediately. For the toxicity assessment of TiO_2 under OS conditions, BRL-3A cells were incubated with H_2O_2 (1–100 μM) for 1 h followed by exposure to TiO_2. Then, all cells were incubated with H_2O_2 and TiO_2 together for 6 h. The effects of TiO_2 on BRL-3A cells in terms of cell viability were assessed to detect the potential changes of toxicity among different cell growth microenvironments.

Analysis of cellular DNA content

The cell cycle has distinct phases with different cellular DNA contents. DNA content analysis can reveal the percentage of cells in G0/G1, S and G2/M. In this study, the DNA content changes of synchronized BRL-3A cells after H_2O_2 and/or NMs exposure was checked by flow cytometry (Kim *et al*., 2012). Briefly, the collected cells were fixed in 75% ice-cold ethanol overnight at 4 °C. Then, the cells were washed with PBS buffer and lysed by RNase A. Propidium iodide (PI, Excitation/Emission = 488/620 nm) was added to the cell lysate. Finally, the percentage of cells in the G0/G1, S and G2/M phase was obtained through a Becton Dickinson FACScalibur flow cytometer (Wang *et al*., 2009b).

Rat groups

All animal experiments and procedures used in this study were approved by the Ethics Committee of Animal Experiments of Xi'an Jiaotong University (Permit Number: XA-20121010), according to the recommendations in the Guide for the Care and Use of Laboratory Animals in our institutes. All surgery was performed under pentobarbital anesthesia with minimum suffering. Healthy male SD rats [Experimental animal center of The Fourth Military Medical University, body weight (BW) of 195 ± 20 g] were housed in stainless-steel cages with 30 lux light intensity, 25 °C room temperature, 60% relative humidity, distilled water and sterilized food. SD rats were randomly divided into six groups: The control group (0.9% normal saline), the NMs group (nano-TiO_2), the MMs group (micro-TiO_2), the OS group (alloxan), the OS-MMs group and the OS-NMs group. The NMs group, MMs group, OS-MMs group and OS-NMs group included three subgroups based on the different dosages (0.5, 5 and 50 mg kg^{-1} BW) of TiO_2. Sterilized TiO_2 was suspended in 0.9% normal saline with a 30-min ultrasonic treatment before use in animal experiments. For the NMs group and MMs group, TiO_2 suspensions were injected slowly and gently into the abdominal cavity of rats and left for 24 h. For the OS group, alloxan (70 mg kg^{-1} BW) was used to induce the OS conditions in rats by gentle intramuscular injection and left for 24–72 h. For the OS-NMs group and OS-MMs group, TiO_2 (0.5-50 mg/kg BW) were injected slowly via i.p. injection after alloxan induced the occurrence of OS conditions in rats.

At the end of experimental procedure, rats were anesthetized by i.p. administration of pentobarbital (45 mg kg^{-1} BW). Blood was collected through a femoral arterial cannula. The sera were obtained from rat whole blood by centrifuge at 2000 *g* for 20 min. Liver tissues were excised for the assessment of OS conditions and histopathological analysis.

Alloxan-induced OS conditions in rats

After homogenization and centrifugation, the components of rat liver tissues in the OS group were used to determine the changes of O_2^-, MDA, SOD and GSH levels, according to previous methods (Bautista *et al*., 1990; Buege and Aust, 1978; Kuo *et al*., 2011; Wang *et al*., 2009b).

Histopathological assay

In histopathological analysis, liver tissues were isolated and fixed using 10% phosphate-buffered formalin for 48 h, and embedded in paraffin. The sections of liver were stained using hematoxylin and eosin (H&E) (Rubin and Lieber, 1974). Digital photomicrographs of tissue sections were examined using an Axiocam HRc camera (Zeiss). Six random fields of each tissue section were selected to analyze pathological changes, according to the definition of grade 2 and 3 hepatic damage, such as hemorrhage, neutrophil infiltration, nuclear pyknosis and the loss of distinct cellular borders (Camargo *et al*., 1997). The percentage of hepatic pathological changes was calculated using Image-Pro Plus 6.0 (Silver Spring, MD, USA) (Anderson *et al*., 2005; Doherty *et al*., 2011).

Biochemical measurements of rat liver damage

As the biomarkers of liver damage, the activities of AST, ALT, LDH and ALP in rat sera were assayed after alloxan and/or nano-TiO_2 injection (Bagchi *et al*., 1995; Osuna *et al*., 1977; Shakoori *et al*., 1994; Tietz, 1976), according to the ELISA kits with the manufacturer's instructions.

Statistical analysis

All results were presented as the mean ± standard deviation (SD). Statistically significant differences were performed using Student's *t*-tests, one-way analysis of variance (ANOVA) and two-way ANOVA with Tukey's *post-hoc* test wherever appropriate. *P*-values less than 0.05 were considered statistically significant.

Results

Characterization of Nano-TiO_2

Based on the TEM and SEM images, nano-TiO_2 showed the rod-like shape with a size of 12–18 nm (diameter) × 40–80 nm (length) (Fig. 1A, B). For the X-ray diffraction (XRD) pattern of nano-TiO_2, strong diffraction peaks were shown at 28°, 36°and 54° (Fig. 1C), which were consistent with a standard spectrum of rutile nano-TiO_2 (Thamaphat *et al*., 2008). Based on XRD results, we analyzed the proportion of the rutile phase, which was 99.92% (Hanaor and Sorrell, 2011). Further, the selected area electron diffraction (SAED) pattern of nano-TiO_2 was in accordance with the XRD data (Fig. 1A), indicating nano-TiO_2 in the rutile phase (Fig. 1D). The crystal lattice plane of nano-TiO_2 was exhibited in a high-resolution TEM (HRTEM) image, showing a 110 crystal lattice plane with 0.313 nm d-spacing (Fig. 1E). The zeta potential of nano-TiO_2 was −41.7 ± 5.4 mV (Fig. 1F). The size distributions of nano-TiO_2 suspended in RPMI 1640 with 10% (v/v) FBS and 0.9% normal saline are shown in Fig. 1G. The surface area of nano-TiO_2 was 150–171 $m^2 g^{-1}$.

Induction of OS conditions in BRL-3A cells

To induce the OS conditions in BRL-3A cells, we incubated cells with 0.01 μM to 10 M of H_2O_2 for 1, 6, 12 and 24 h. We observed that cell viability was significantly reduced at all four incubation periods when cells were exposed to H_2O_2 concentrations

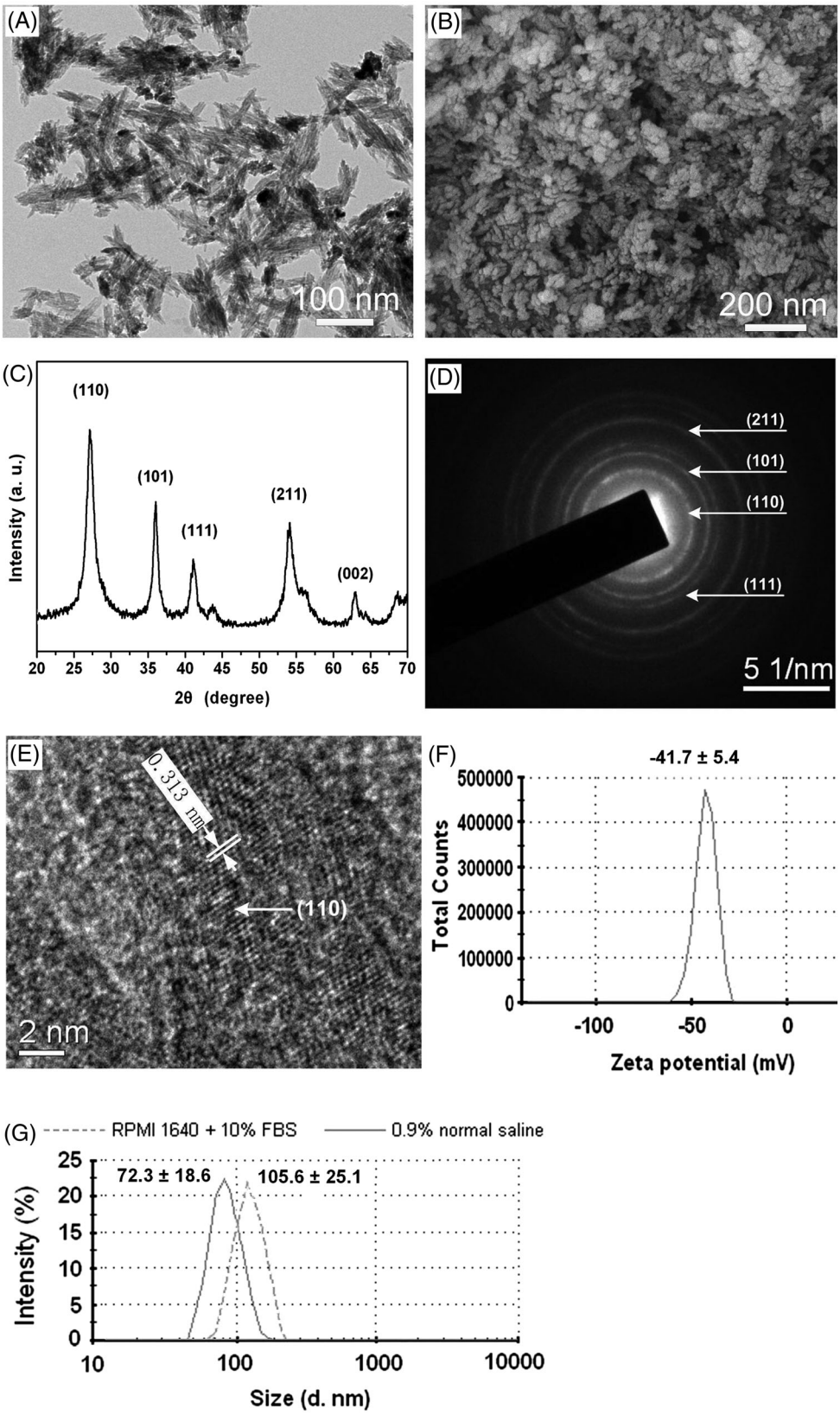

Figure 1. Characterization of nano-titanium dioxide (TiO_2). (A) Transmission electron microscopy (TEM) image of ethanol-dispersible nano-TiO_2; (B) scanning electron microscope (SEM) image of nano-TiO_2; (C) X-ray diffraction (XRD) pattern of nano-TiO_2; (D) selected area electron diffraction (SAED) pattern of nano-TiO_2; (E) high-resolution transmission electron microscopy (HRTEM) image of nano-TiO_2; (F) zeta potential of nano-TiO_2 (0.1 mg ml^{-1}), the value was the average of 15 runs of 30 measurements; (G) size distribution of nano-TiO_2 (0.1 mg ml^{-1}), the data were the average of 15 runs of 20 measurements. Nano-TiO_2 were suspended in 0.9% normal saline with 30-min ultrasonic treatment before the measurement of size distribution. Nano-TiO_2 were incubated in RPMI 1640 with 10% fetal calf serum (FBS) (0.1 mg ml^{-1}) for 24 h at 37 °C before the measurement of size distribution.

Journal of Applied Toxicology

above 1 mM (1–24 h) (Fig. 2). Further, viabilities of BRL-3A cells obtained at 1, 10, 100 mM, 1 and 10 M of H_2O_2 demonstrated that H_2O_2 induced the cytotoxicity in a time-dependent manner, which exhibited a significant reduction in cell viability ($P < 0.05$) from $87.8 \pm 5.0\%$, $63.1 \pm 1.6\%$, $13.1 \pm 1.5\%$, $11.6 \pm 1.$ 7% and 7.9 ± 0.9 % after 1-h incubation to $53.3 \pm 4.8\%$, 29.9 ± 8.1 %, 8.9 ± 2.6 %, 5.5 ± 3.1 % and 3.9 ± 3.1 % after 24 h, respectively

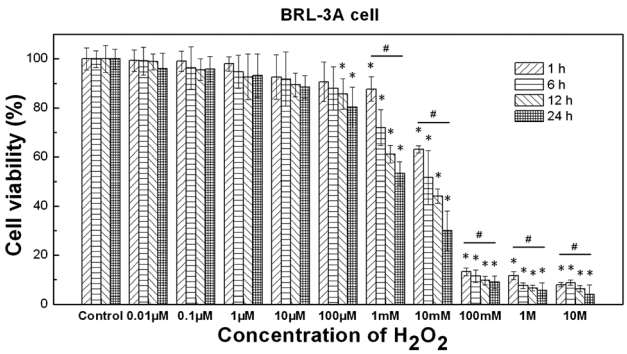

Figure 2. Changes in BRL-3A cell viability after hydrogen peroxide (H_2O_2) exposure. Ten concentrations of H_2O_2 (0.01 μM to 10 M) and four incubation periods (1–24 h) were used to explore the effects of H_2O_2 in BRL-3A cells. After BRL-3A cells were incubated with H_2O_2, cell viability was measured using the MTT assay. Based on the observed insignificant reduction of cell viabilities after 1 hr H_2O_2 exposure, the concentrations of H_2O_2 lower than 100 μM were suggested to induce OS conditions in BRL-3A cells. $^{*}P < 0.05$, compared with the related control at each incubation time (1, 6, 12 and 24 h) (one-way ANOVA, Tukey's *post hoc* test); $^{\#}P < 0.05$, comparison amongst results of 1- to 24-h exposure times at each concentration of H_2O_2 (one-way ANOVA); $n = 6$.

(Fig. 2). Importantly, 0.01–100 μM of H_2O_2 induced insignificant cytotoxicity after 1-h exposure, indicating that these concentrations of H_2O_2 can be used to mimic the OS conditions in BRL-3A cells without causing a significant effect on cell viability.

To ensure the OS conditions in BRL-3A cells, we checked the changes in O_2^-, MDA, SOD and GSH levels after 0.01–100 μM of H_2O_2 exposure (1 h) (Fig. 3). We observed a significant increase in O_2^- and MDA contents and a reduction in SOD and GSH levels when the H_2O_2 concentrations were higher than 1 μM, compared with the H_2O_2-free cell control. These results demonstrated that H_2O_2 resulted in the OS conditions in BRL-3A cells. Thus, we selected 1, 10 and 100 μM of H_2O_2 and a 1-h exposure period to induce the OS conditions (without significant effects of cell viability) in subsequent cellular toxicity experiments.

Adverse effects of TiO_2 under OS conditions in BRL-3A cells

To evaluate the adverse effects of TiO_2, we checked BRL-3A cell viability after 0.1, 1, 10 and 100 μg ml^{-1} of microscale and nanoscale TiO_2 exposure under OS conditions. Based on our previous results, nano-TiO_2 did not significantly reduce viabilities of normal BRL-3A cells at these four concentrations when the incubation time was less than 6 h (Supplementary Fig. 1). However, one-way ANOVA analysis showed that nano-TiO_2 exposure led to cytotoxicity in a concentration-dependent manner under OS conditions (1–100 μM) (Fig. 4). For example, compared with normal cells after NMs exposure, the viabilities of BRL-3A cells with OS conditions (100 μM H_2O_2) significant decreased to $80.1 \pm 3.5\%$, 76.7 ± 8.7 %, 75.1 ± 6.8 % and $74.9 \pm 6.3\%$ after exposure to 0.1, 1, 10 and 100 μg ml^{-1} of NMs, respectively (Fig. 4). Furthermore, cell viabilities decreased with the increase in H_2O_2 concentrations when BRL-3A cells were exposed to an equivalent concentration

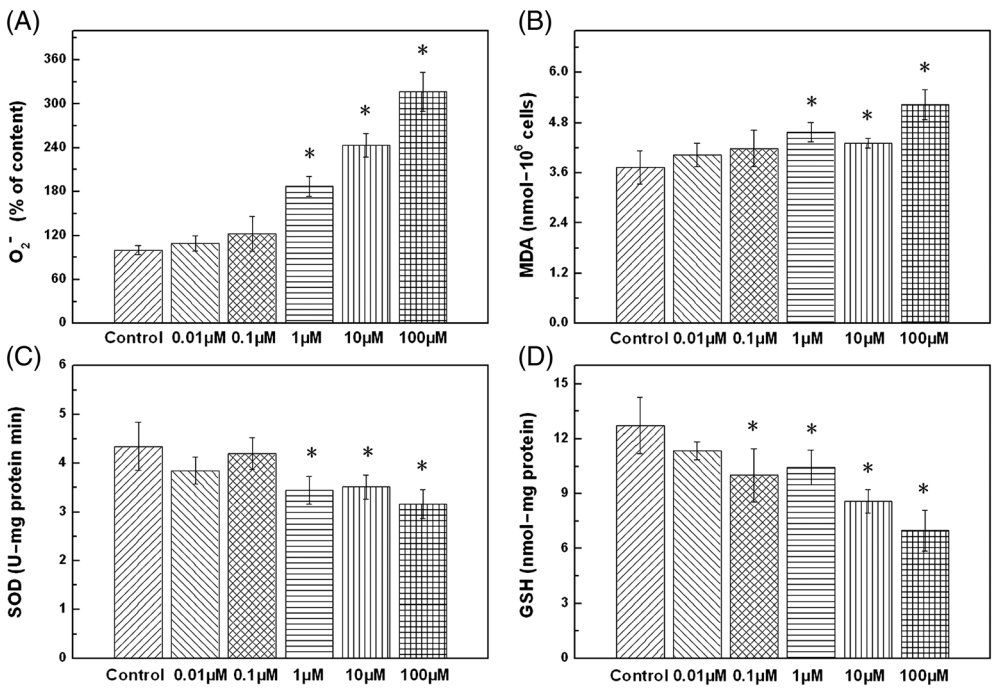

Figure 3. Changes in oxidative stress (OS) indexes in BRL-3A cells after 1-h hydrogen peroxide (H_2O_2) exposure. To detect the OS conditions induced by 0.01–100 μM of H_2O_2, the levels of intracellular O_2^-, malondialdehyde (MDA), superoxide dismutase (SOD) and glutathione (GSH) were measured. Significant changes in four OS indexes were obtained when the concentrations of H_2O_2 were above 1 μM. $^{*}P < 0.05$, compared with the related control of each OS index (one-way ANOVA, Tukey's *post hoc* test) , $n = 6$.

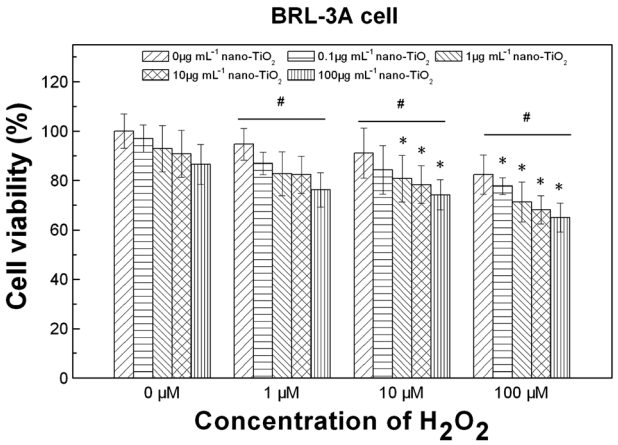

Figure 4. Changes in BRL-3A cell viability after nano-titanium dioxide (TiO_2) exposure under oxidative stress (OS) conditions. Nano-TiO_2 (0.1–100 μg ml^{-1}) were added to BRL-3A cells for 6 h after they were incubated with hydrogen peroxide (H_2O_2) (1–100 μM) for 1 h. The H_2O_2 exposure time in controls was 7 h. $^{*}P < 0.05$, compared with the related control (H_2O_2-free) at the same exposed concentration of nano-TiO_2 (0.1, 1, 10 or 100 μg ml^{-1}) (one-way ANOVA, Tukey's *post hoc* test); $^{\#}P < 0.05$, comparison amongst results of nano-TiO_2 (0–100 μg ml^{-1}) exposure at each concentration of H_2O_2 (one-way ANOVA); $n = 6$.

of nano-TiO_2. For example, the loss of BRL-3A cells enhanced by 2.39 ± 0.18, 2.48 ± 0.21 and 3.72 ± 0.09 fold after 1, 10 and 100 μM of H_2O_2 exposure at 100 μg ml^{-1} of nano-TiO_2, respectively (Fig. 4). For micro-TiO_2, compared with H_2O_2-treated controls, the cell viability of BRL-3A cells showed no significant changes after 0.1, 1, 10 and 100 μg ml^{-1} of micro-TiO_2 exposure under OS condition (Supplementary Fig. 2).

Effect of Nano-TiO_2 on cell cycle distribution in BRL-3A cells

To investigate the potential mechanism of nano-TiO_2 toxicity under OS conditions, we checked the cell-cycle distribution using flow cytometry. The cell cycle is shown with three phases based on DNA content, including the G0/G1 (resting/growth) phase, the S (DNA synthesis) phase and the G2/M (division) phase. Based on the significant cytotoxicity of nano-TiO_2 (0.1–100 μg ml^{-1}) under OS conditions (Fig. 4), we analyzed the changes in cell cycle distribution after 100 μM of H_2O_2 exposure (Fig. 5). Compared with the normal BRL-3A cells, 100 μM of H_2O_2 (NMs free) inhibited the G0/G1 phase to the S phase transition (Fig. 5 F), which was similar to the effects of nano-TiO_2 (above 1 μg ml^{-1}, H_2O_2 free) on the cell cycle distribution in normal cells (Fig. 5C–E). However, nano-TiO_2 prevented normal cells from entering the S phase, which was opposite to their role in cells under OS conditions (Fig. 5G–J). Compared with the NMs exposed normal cells (Fig. 5B–E), the accumulation of G0/G1 phase arrest was attenuated after nano-TiO_2 exposure under OS conditions, which accelerated G0/G1 progression to the S phase (0.1–100 μg ml^{-1} of nano-TiO_2) and significantly enhanced G2/M phase arrest (10–100 μg ml^{-1} of nano-TiO_2). For the G0/G1 phase, two-way ANOVA analysis exhibited a significant effect of H_2O_2 [$F_{(1,50)} = 38.13$, $P = 4.94 \times 10^{-6}$] but not TiO_2 NMs [$F_{(4,50)} = 2.09$, $P = 0.12$], and a significant interaction [$F_{(4,50)} = 57.92$, $P = 1.03 \times 10^{-10}$]. For the S phase, two-way ANOVA revealed a significant effect of TiO_2 NMs [$F_{(4,50)} = 5.04$, $P = 0.006$] but not H_2O_2 [$F_{(1,50)} = 0.40$, $P = 0.54$], and a significant interaction [$F_{(4,50)} = 22.86$, $P = 3.20 \times 10^{-7}$]. For the G2/M phase, two-way ANOVA results showed a significant effect of H_2O_2 [$F_{(1,50)} = 37.67$, $P = 5.37 \times 10^{-6}$] but not TiO_2 NMs [$F_{(4,50)} = 2.71$, $P = 0.059$], and a significant interaction [$F_{(4,50)} = 27.71$, $P = 6.61 \times 10^{-8}$]. These results suggested that the synergistic interaction of 100 μM H_2O_2 with nano-TiO_2 affected the changes of cell cycle distribution.

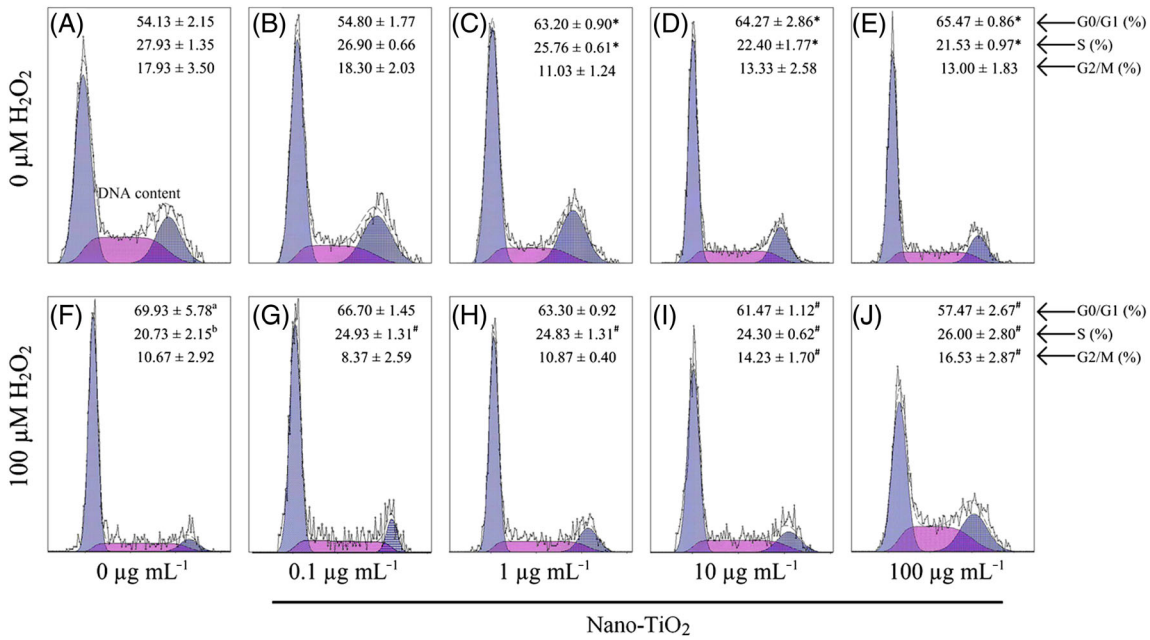

Figure 5. Cell cycle distribution in normal and oxidative stress (OS) BRL-3A cells after nano-titanium dioxide (TiO_2) exposure. DNA content was measured by flow cytometry. (A)–(E) Normal BRL-3A cells were exposed to nano-TiO_2 (0.1–100 μg ml^{-1}) for 7 h. (F)-(J) Cells were exposed to nano-TiO_2 (0.1–100 μg ml^{-1}, 6 h) after H_2O_2 (100 μM, 1 h) incubation. [a] G0/G1 phase, [b] S phase, $P < 0.05$, comparison between normal cells and OS-cells (100 μM of H_2O_2) without NMs exposure. $^{*}P < 0.05$, compared with the related control of each phase in normal cell cycle (G0/G1 phase, S phase or G2/M phase); $^{\#}P < 0.05$, compared with the related control of each phase in OS cells (100 μM H_2O_2 incubation); one-way ANOVA, Tukey's *post hoc* test; $n = 6$.

Journal of Applied Toxicology

OS conditions in rats

To further examine the effects of TiO_2 under OS conditions, we performed animal test using a SD rat as the animal model. We used alloxan to induce OS conditions in rats, measuring the content or level changes of O_2^-, MDA, SOD and GSH after alloxan injection (Fig. 6). The significant increase in O_2^- and MDA contents and reduction in SOD and GSH levels were obtained after 24-h injection of alloxan, and the occurrence of OS conditions in rats lasted for at least 72 h. However, we observed histopathological changes and a significant difference in liver damage biomarkers (AST, ALT, LDH and ALP) in rat sera after 72-h alloxan injection (Supplementary Fig. 3), suggesting that alloxan led to liver damage in rats. Based on the above results, rats i.p. injected with TiO_2 (0.5–50 mg kg^{-1} BW) for 24 h were selected to perform the acute toxicity experiments after 24-h alloxan treatments. The total exposure time of alloxan was 48 h, excluding the negative influences of alloxan to liver tissues.

Histopathological assay of rat liver

To explore the liver damage after TiO_2 injection, we further checked the histopathological characteristics of liver tissues under normal and OS conditions (Fig. 7). In the NMs subgroups and OS-NMs subgroups, liver damage was worse with the increasing dosages of nano-TiO_2. Under healthy conditions, we observed histopathological changes when the dosages of nano-TiO_2 were higher than 5 mg kg^{-1} BW. These changes included cell infiltration (Fig. 7C) and hepatocyte necrosis (Fig. 7D). In contrast, hepatic histopathological changes appeared at the lowest dosages (0.5 mg kg^{-1} BW) of NMs and became obvious at high dosages of NMs under OS conditions (Fig. 7 F). Further, we quantified the percentages of pathological changes, which showed the significant difference between alloxan-treated and healthy rats when NMs dosage was 50 mg kg^{-1} BW (Fig. 7I). However, based on H&E images of rat livers, micro-TiO_2 did not induce the obvious hepatic pathological changes in healthy or alloxan-treated rats, even after 50 mg kg^{-1} BW of micro-TiO_2 exposure (Supplementary Fig. 4). Then, all these indicated that OS conditions led to increased lesions of rat liver with increasing NMs dosages.

Changes of liver damage biomarkers in rats

To confirm the liver damage induced by nano-TiO_2 under OS conditions, we measured the activities of liver damage biomarkers in rat sera (i.e. AST, ALT, LDH and ALP). The activities of AST (Fig. 8A), ALT (Fig. 8B), LDH (Fig. 8C) and ALP (Fig. 8D) in alloxan-induced rats were significant higher than healthy rats after 0.5, 0.5, 50 and 0.5 mg kg^{-1} BW injection of nano-TiO_2. For example, compared with healthy rats, there was 1.19 ± 0.11, 1.43 ± 0.27 and 1.37 ± 0.32 folds increase in the activity of AST in OS rats after receiving 0.5, 5 and 50 mg kg^{-1} BW of nano-TiO_2, respectively. Results of two-way ANOVA analyzes suggested that the synergistic interactions of OS conditions and nano-TiO_2 significantly enhanced the hepatotoxicity *in vivo* compared with the individual effect of nano-TiO_2 (Supplementary Table S1), coinciding the results of histopathological changes in healthy and alloxan-treated rats (Fig. 7).

Discussion

In this study, we investigated the hepatotoxicity of nanoscale and microscale TiO_2 under OS conditions both *in vitro* and *in vivo*. Our *in vitro* results suggested that the interactions between OS conditions and nano-TiO_2 significantly increased nanotoxicity in cultured liver cells, compared with NMs exposure only. The presence of OS conditions enhanced cytotoxicity (reduced cell viability) in BRL-3A cells when exposed to various

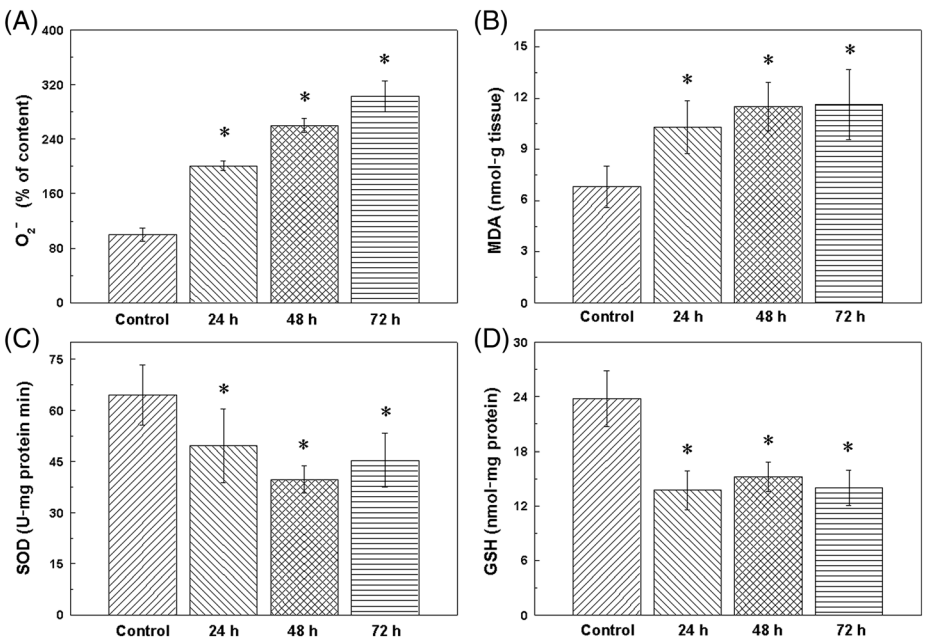

Figure 6. Changes of oxidative stress (OS) indexes in rat sera after alloxan injection. Levels of O_2^-, malondialdehyde (MDA), superoxide dismutase (SOD) and glutathione (GSH) in rat sera were measured after intraperitoneal injection of alloxan [70 mg kg^{-1} body weight (BW)] for 24, 48 and 72 h. $^*P < 0.05$, compared with the related control of each OS index (one-way ANOVA, Tukey's *post hoc* test), $n = 6$.

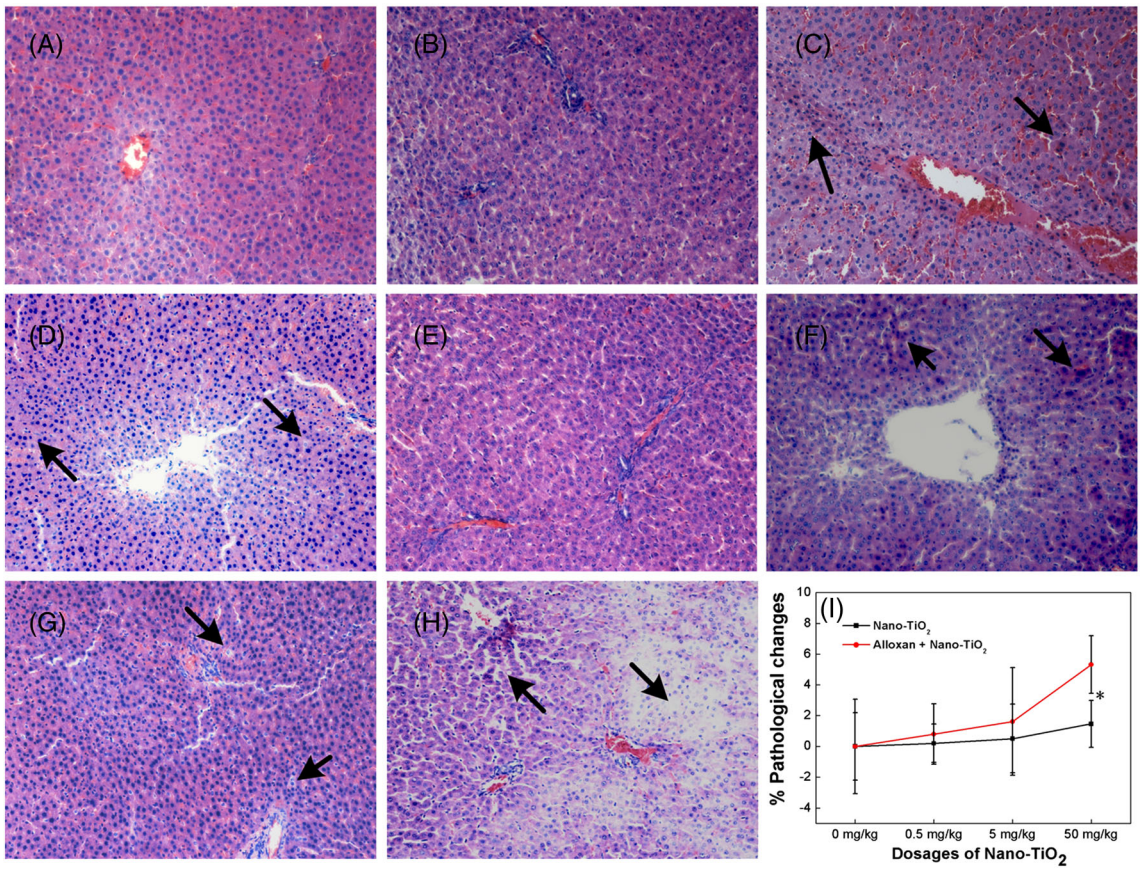

Figure 7. Histopathology of rat liver after alloxan and/or nano-titanium dioxide (TiO_2) exposure. (A–J) hematoxylin and eosin (H&E) stain, 200×. (A) Control (24 h): normal appearance of the liver; (B) 0.5 mg kg^{-1} nano-TiO_2: normal appearance of the liver; (C) 5 mg kg^{-1} nano-TiO_2: cell infiltration (arrows); (D) 50 mg kg^{-1} nano-TiO_2: hepatocyte necrosis (arrows); (E) Alloxan (48 h): normal appearance of the liver; (F) Alloxan + 0.5 mg kg^{-1} nano-TiO_2: cell infiltration (arrows); (G) Alloxan + 5 mg kg^{-1} nano-TiO_2: hepatocyte necrosis (arrows); (H) Alloxan + 50 mg kg^{-1} nano-TiO_2: hepatocyte necrosis and destruction of hepatic architecture (arrows); (I) Representative micrographs of H&E-stained liver were selected to calculate the pathological changes by Image-Pro Plus 6.0. The significant difference in pathological change proportion between the NMs group and OS-NMs group were analyzed ($^{*}P < 0.05$, Student's *t*-test).

concentrations of nano-TiO_2, which may be caused by the synergistic effects of nano-TiO_2 and OS conditions upon cell cycle distribution (Fig. 5). In addition, *in vivo* experiments showed more obvious hepatic pathological changes and elevated activities of AST, ALT, LDH and ALP in rats under alloxan-induced OS conditions than healthy rats after nano-TiO_2 exposure (Figs 7 and 8). Compared with the no toxic effect of micro-TiO_2, the synergistic interactions of OS conditions and nano-TiO_2 *in vitro* or *in vivo* could enhance adverse effects relative to those individually under normal/healthy conditions.

Physicochemical properties of NMs were important during the assessments of nanotoxicity. The shape of nano-TiO_2 was rod like in this study, which was similar to the morphology of commercially available pigment particles (231 ± 93 nm) (Hussain *et al.*, 2012). Rod-like particles can enhance an adverse effect through evading phagocyte-mediated clearance or aggregation (Brown *et al.*, 2007), such as TiO_2 nanobelts (15–30 μm long, 60–300 nm wide) led to significant cytotoxicity in alveolar macrophage compared with TiO_2 nanospheres (diameter 60–200 nm) (Hamilton *et al.*, 2009). In addition, based on the DLS results, the sizes of nano-TiO_2 were different after being suspended in culture medium and saline. Compared with the dimension of NMs in 0.9% normal saline, the components in RPMI 1640 culture medium (with 10% FBS) led to an increase of nano-TiO_2 size, as observed in CdSe-ZnS quantum dots (Galeone *et al.*, 2012; Maiorano *et al.*, 2010). There was no change in the shape and size of nano-TiO_2 after 24-h incubation with 100 μM H_2O_2 (data not shown).

OS conditions were induced by H_2O_2 and alloxan in BRL-3A cells and rat livers (Wang *et al.*, 2008; Wexler 1981), respectively. H_2O_2 is a naturally produced by-product of oxidative metabolism (Campbell *et al.*, 2001). The excessive H_2O_2 can lead to the risk of OS in human lens epithelial cells (50 μM H_2O_2 for 1–8 h) (Goswami *et al.*, 2003) and intense airway inflammation in guinea pigs (10–1000 mM for 10 min) (Misawa and Arai, 1993). Furthermore, the concentrations of H_2O_2 used in our cytotoxicity experiments were similar to levels in freshly voided human urine (0.4–109.6 μM) (Halliwell *et al.*, 2000) and concentrations in the inflammatory phase of murine cutaneous wounds (0.1–0.2 mM) (Roy *et al.*, 2006). Alloxan (2,4,5,6-pyrimidinetetrone) can selectively destroy insulin-producing pancreatic beta cells in rodents, inducing diabetes through the generation of ROS in a cyclic reaction with dialuric acid (Szkudelski, 2001). A previous study showed that 70 mg kg^{-1} BW alloxan induced diabetes after 72-h injection in albino rats (Sciences *et al.*, 2007).

As an endpoint of OS condition, the activity of SOD was reduced after H_2O_2 and alloxan treatment. SOD is one important component of the antioxidant defense system, which leads to

Journal of AppliedToxicology

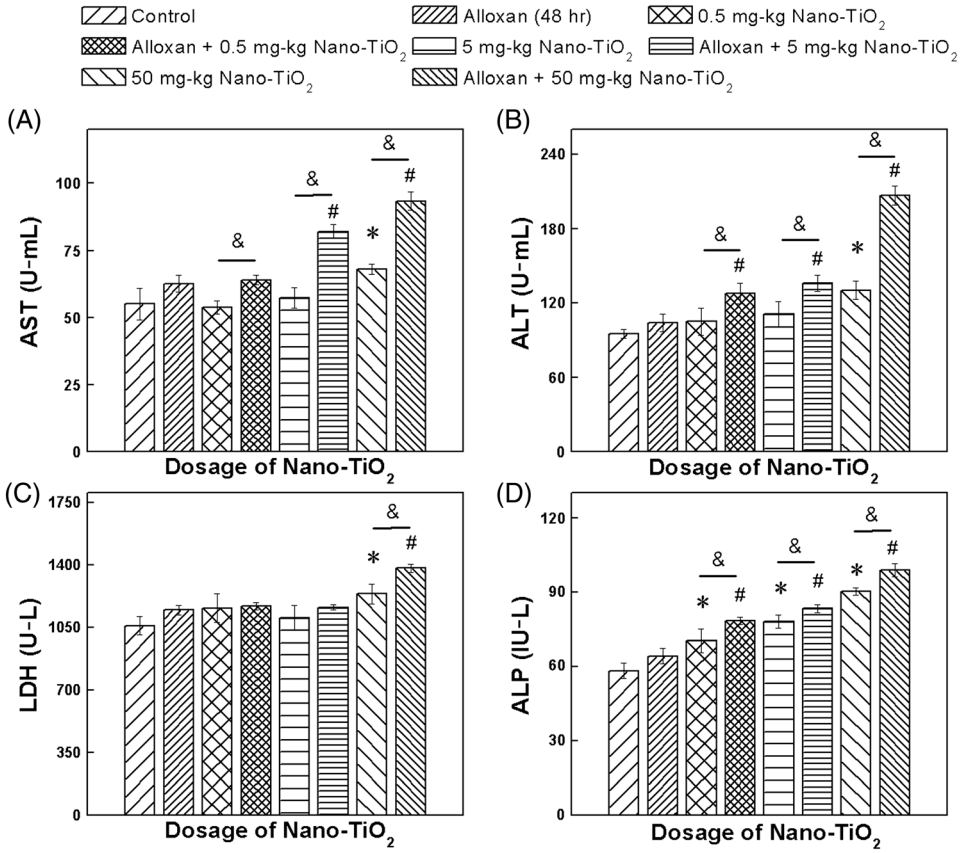

Figure 8. Changes in rat liver biomarkers after alloxan and/or nano-titanium dioxide (TiO_2) injection. Aspartate aminotransferase (AST) (A), alanine aminotransferase (ALT) (B), lactate dehydrogenase (LDH) (C) and alkaline phosphatase (ALP) (D), as the biochemical markers of liver damage, were monitored after 24-h nanomaterials (NMs) injection with/without oxidative stress (OS) conditions. $^{*}P < 0.05$, compared with control (one-way ANOVA, Tukey's *post hoc* test); $^{\#}P < 0.05$, compared with alloxan (48 h) (one-way ANOVA, Tukey's *post hoc* test); $^{\&}P < 0.05$, comparison between activities of liver biomarkers in healthy rats and OS rats after nano-TiO_2 exposure, Student's *t*-test; $n = 6$.

the dismutation of O_2^- into H_2O_2 and O_2 (Fridovich, 1995). Previous studies have confirmed that the SOD activity can increase first and then decreases after periods of exposure to H_2O_2 (Lassoued *et al*., 2010; Vu *et al*., 2012). For example, 10 μM H_2O_2 enhanced SOD activity after 2-h treatment, whereas H_2O_2 reduced SOD activity at 24 h in cultured bovine luteal endothelial cells (Vu *et al*., 2012). In addition, some investigators have demonstrated that diabetes mellitus (OS conditions) can decrease the SOD activity (Cohen, 1995; Loven *et al*., 1986; Wohaieb and Godin, 1987). As SOD decreases after H_2O_2 or alloxan treatment, Karasu (1999) speculated that increased generation of oxygen-derived free radicals reduced the activity of SOD, resulting in an increase in O_2. As a consequence of increased production of O_2^-, a continuous increase of ·OH production can result in a decrease in SOD activity through a negative feedback mechanism (product inhibition) (Chang *et al*., 1993; Hunt *et al*., 1988).

Several potential mechanisms have been suggested to explain the cytotoxicity of NMs *in vitro*, such as the changes of cell cycle distribution. Based on our cell cycle analysis (Fig. 5), NMs-free normal cells were readily arrested in the G0/G1 phase after 100 μM H_2O_2 exposure, which was in accordance with the effects of peroxides in human fibroblasts and Chinese hamster ovary cells (Clopton and Saltman, 1995; Shackelford *et al*., 2001). Single exposure of nano-TiO_2 also arrested BRL-3A cells in the G0/G1 phase in a concentration-dependent manner. TiO_2 nanotoxicity in normal BRL-3A cells enhanced G0/G1 phase arrest, which may not only maintain the non-proliferative status of cells (Chapman *et al*., 2000) but also induce DNA damage, abnormal DNA synthesis, and decrease the cell number in the S phase (Li *et al*., 2010; Trouiller *et al*., 2009). However, compared with the only NMs exposed normal cells, nano-TiO_2 accelerated the transition from G0/G1 to the S phase under OS conditions. Importantly, OS conditions and nano-TiO_2 synergistically provoked G2/M phase arrest (Fig. 5). The synergistic interaction between OS conditions and nano-TiO_2 may activate the functions of factors such as clusterin, which can induce G2/M arrest and apoptosis (Scaltriti *et al*., 2004).

Acute toxicity of nano-TiO_2 to SD rat liver under OS conditions was observed simultaneously, because BRL-3A cells can lose the biological function rapidly when cells are maintained *in vitro* and the lack of biological function may affect the cells' response to toxin (Boess *et al*., 2003; Casley *et al*. 1995). The enhanced adverse effects caused by NMs under OS conditions *in vivo* were shown and maybe as a result of aggravating pathological changes (necrosis and dysfunction) of liver tissue, which was coincident with the increased sensitivity to endotoxin liver damage in obese animals (Yang *et al*., 1997). The increase in LDH and ALP is considered as a result of progressive liver necrosis (Bagchi *et al*., 1995; Tietz, 1976). The leakage from hepatocyte

can enter the blood stream when liver dysfunction, which can increase activities of AST and ALT enzymes (Navarro *et al.*, 1993; Shakoori *et al.*, 1994). Severe hepatocellular death and liver dysfunction can lead to acute liver failure (Malhi *et al.*, 2006), which shows an important relationship to rapidly progressive hepatic encephalopathy, leading to devastating complications (Bernal *et al.*, 2010).

Slight to severe changes in liver pathology in OS rats were obtained after 0.5–50 mg kg^{-1} BW nano-TiO_2 exposure. The maximum dose of nano-TiO_2 used in the acute toxicity assessment of OS rat livers was 50 mg kg^{-1} BW, which was less than the doses in other relative studies of healthy rats (560–1000 mg kg^{-1} BW) (Fabian *et al.*, 2008; Warheit *et al.*, 2007). This dosage could be viewed as 3.5 g nano-TiO_2 for 70-kg sick humans with such an exposure. Although some people think that 50 mg kg^{-1} BW might be an unreachable daily dosage, we should take the accumulation effect of NMs into consideration, because the clearance rate of NMs may be very slow after exposure to NMs containing air, foods and daily necessities (Christensen *et al.*, 2011). For instance, most of the 40-nm gold nanoparticles will remain in the liver during the mice life span after i.v. injections (Sadauskas and others 2009). The concentration of nano-TiO_2 (< 100 nm) in the rat liver was retained for at least 28 days after a 5 mg kg^{-1} BW injection (Fabian *et al.*, 2008). For human beings, an epidemiological cohort study from six European countries indicated a significantly increased risk of lung cancer in workers in the nano-TiO_2 production industry than the general population, although the estimated average exposure of workers was less than the permissible exposure limits of occupational safety and health administration (15 mg m^{-3}) and immediately dangerous to life or health concentrations (7500 mg m^{-3}) for nano-TiO_2 (Baan *et al.*, 2006; Zhang *et al.*, 2011).

Nowadays, approximately 250 nanomedicine products are being assessed in humans, and most of them are used as imaging, diagnostics and vehicles for drugs to treat diseases (Marshall, 2011). Many researchers think that the NMs are non-toxic in a healthy body; for example, quantum dots showed no adverse response to healthy non-human primates after 90 days i.v. injection (25 mg kg^{-1} BW) (Ye *et al.*, 2012). Even so, clinical trials in patients are still not subject to standardized oversight of adverse effects of NMs (Marshall, 2011), which become ever more necessary and specialized to future nanomedicine.

Conclusions

In summary, to evaluate the nanotoxicity under OS conditions, we studied the adverse effects of TiO_2 in BRL-3A cells and SD rat livers. The synergistic effect of H_2O_2 with nano-TiO_2 enhanced the cytotoxicity *in vitro* through the abnormal G0/G1 and S phase transition and G2/M arrest. *In vivo*, the alloxan-induced OS rats showed obvious hepatic pathological changes, and significant increased activities of hepatic damage indicators when the dosage of nano-TiO_2 was increased. This study suggests the importance of NMs-induced toxicity in diseased status, which should be carefully considered when patients are exposed to NMs-containing products.

Conflict of Interest

The authors declare that there are no conflicts of interest.

SUPPORTING INFORMATION

Supporting information can be found in the online version of this article.

Acknowledgements

This work was supported by the National "111 Project" Foundation of China (Grant No. B06024), the Major International Joint Research Program of China (11120101002), Key Project of Chinese Ministry of Education (313045), Projects of International Cooperation and Exchanges NSFC (2013DFG02930), Program for New Century Excellent Talents in University (NCET-12-0437).

References

Anderson CD, Pierce J, Nicoud I, Belous A, Knox CD, Chari RS. 2005. Modulation of mitochondrial calcium management attenuates hepatic warm ischemia-reperfusion injury. *Liver Transpl.* **11**: 663–668. DOI: 10.1002/lt.20407.

Asakura M, Sasaki T, Sugiyama T, Takaya M, Koda S, Nagano K, Arito H, Fukushima S. 2010. Genotoxicity and cytotoxicity of multi-wall carbon nanotubes in cultured Chinese hamster lung cells in comparison with chrysotile A fibers. *J. Occup. Health* **52**: 155–166. DOI: 10.1310/hpj4405-401.

Baan R, Straif K, Grosse Y, Secretan B, El Ghissassi F, Cogliano V. 2006. Carcinogenicity of carbon black, titanium dioxide, and talc. *Lancet Oncol.* **7**: 295–296. DOI: 10.1016/S1470-2045(06)70651-9.

Bagchi D, Bagchi M, Hassoun EA, Stohs SJ. 1995. In vitro and *in vivo* generation of reactive oxygen species, DNA damage and lactate dehydrogenase leakage by selected pesticides. *Toxicology* **104**: 129–140. DOI: 10.1016/0300-483X(95)03156-A.

Bautista AP, Meszaros K, Bojta J, Spitzer JJ. 1990. Superoxide anion generation in the liver during the early stage of endotoxemia in rats. *J. Leukocyte Biol.* **48**: 123–128.

Bernal W, Auzinger G, Dhawan A, Wendon J. 2010. Acute liver failure. *Lancet* **376**: 190–201. DOI: 10.1016/S0140-6736(10)60274-7.

Boess F, Kamber M, Romer S, Gasser R, Muller D, Albertini S, Suter L. 2003. Gene expression in two hepatic cell lines, cultured primary hepatocytes, and liver slices compared to the *in vivo* liver gene expression in rats: possible implications for toxicogenomics use of in vitro systems. *Toxicol. Sci.* **73**: 386–402.

Brown SC, Kamal M, Nasreen N, Baumuratov A, Sharma P, Antony VB, Moudgil BM. 2007. Influence of shape, adhesion and simulated lung mechanics on amorphous silica nanoparticle toxicity. *Adv. Powder Technol.* **18**: 69–79. DOI: 10.1163/156855207779768214.

Buege JA, Aust SD. 1978. Microsomal lipid peroxidation. *Methods Enzymol.* **52**: 302–310.

Camargo CA Jr, Madden JF, Gao W, Selvan RS, Clavien PA. 1997. Interleukin-6 protects liver against warm ischemia/reperfusion injury and promotes hepatocyte proliferation in the rodent. *Hepatology* **26**: 1513–1520. DOI: 10.1002/hep.510260619.

Campbell A, Smith MA, Sayre LM, Bondy SC, Perry G. 2001. Mechanisms by which metals promote events connected to neurodegenerative diseases. *Brain Res. Bull.* **55**: 125–132. DOI: 10.1016/S0361-9230(01)00455-5.

Casley WL, Neu JM, Huang HS. 1995. Induction of CYP3A and associated terfenadine N-dealkylation in rat hepatocytes cocultnred with 3 T3 cells. *Health (San Francisco)* **11**: 313–327. DOI: 10.1007/BF01305904.

Chang KC, Chung SY, Chong WS, Suh JS, Kim SH, Noh HK, Seong BW, Ko HJ, Chun KW. 1993. Possible Superoxide Radical-Induced Alteration of Vascular Reactivity in Aortas from Streptozotocin-Treated Rats. *J. Pharmacol. Exp. Ther.* **266**: 992–1000.

Chapman GB, Durante W, Hellums JD, Schafer AI. 2000. Physiological cyclic stretch causes cell cycle arrest in cultured vascular smooth muscle cells. *Am. J. Physiol. Heart Circ. Physiol.* **278**: H748–754.

Chen HW, Su SF, Chien CT, Lin WH, Yu SL, Chou CC, Chen JJ, Yang PC. 2006. Titanium dioxide nanoparticles induce emphysema-like lung injury in mice. *FASEB J.* **20**: 2393–2395. DOI: 10.1096/fj.06-6485fje.

Chen X, Mao SS. 2007. Titanium dioxide nanomaterials: synthesis, properties, modifications, and applications. *Chem. Rev.* **107**: 2891–2959. DOI: 10.1021/cr0500535.

Journal of Applied Toxicology

Christensen FM, Johnston HJ, Stone V, Aitken RJ, Hankin S, Peters S, Aschberger K. 2011. Nano-TiO2-feasibility and challenges for human health risk assessment based on open literature. *Nanotoxicology* **5**: 110–124. DOI: 10.3109/17435390.2010.504899.

Clopton DA, Saltman P. 1995. Low-Level oxidative stress causes cell-cycle specific arrest in cultured cells. *Biochem. Biophys. Res. Commun.* **210**: 189–196. DOI: 10.1006/bbrc.1995.1645.

Codoner-Franch P, Boix-Garcia L, Simo-Jorda R, Del Castillo-Villaescusa C, Maset-Maldonado J, Valls-Belles V. 2010. Is obesity associated with oxidative stress in children? *Int. J. Pediatr. Obes.* **5**: 56–63. DOI: 10.3109/17477160903055945.

Cohen RA. 1995. The role of nitric oxide and other endotheliumderived vasoactive substances in vascular disease. *Prog. Cardiovasc. Dis.* **38**: 105–128.

Desai KM, Chang TJ, Wang H, Banigesh A, Dhar A, Liu JH, Untereiner A, Wu LY. 2010. Oxidative stress and aging: Is methylglyoxal the hidden enemy? *Can. J. Physiol. Pharmacol.* **88**: 273–284. DOI: 10.1139/Y10-001.

Doherty TA, Soroosh P, Khorram N, Fukuyama S, Rosenthal P, Cho JY, Norris PS, Choi H, Scheu S, Pfeffer K, Zuraw BL, Ware CF, Broide DH, Croft M. 2011. The tumor necrosis factor family member LIGHT is a target for asthmatic airway remodeling. *Nat. Med.* **17**: 596–603. DOI: 10.1038/nm.2356.

Dut R, Dizdar EA, Birben E, Sackesen C, Soyer OU, Besler T, Kalayci O. 2008. Oxidative stress and its determinants in the airways of children with asthma. *Allergy* **63**: 1605–1609. DOI: 10.1111/j.1398-9995.2008.01766.x.

Fabian E, Landsiedel R, Ma-Hock L, Wiench K, Wohlleben W, van Ravenzwaay B. 2008. Tissue distribution and toxicity of intravenously administered titanium dioxide nanoparticles in rats. *Arch. Toxicol.* **82**: 151–157. DOI: 10.1007/s00204-007-0253-y.

Fridovich I. 1995. Superoxide radical and superoxide dismutases. *Annu. Rev. Biochem.* **64**: 97–112. DOI: 10.1146/annurev.bi.64.070195.000525.

Galeone A, Vecchio G, Malvindi MA, Brunetti V, Cingolani R, Pompa PP. 2012. *In vivo* assessment of CdSe-ZnS quantum dots: coating dependent bioaccumulation and genotoxicity. *Nanoscale* **4**: 6401–6407. DOI: 10.1039/c2nr31826a.

Ghosh M, Bandyopadhyay M, Mukherjee A. 2010. Genotoxicity of titanium dioxide (TiO_2) nanoparticles at two trophic levels plant and human lymphocytes. *Chemosphere* **81**: 1253–1262. DOI: 10.1016/j.chemosphere.2010.09.022.

Goswami S, Sheets NL, Zavadil J, Chauhan BK, Bottinger EP, Reddy VN, Kantorow M, Cvekl A. 2003. Spectrum and range of oxidative stress responses of human lens epithelial cells to H_2O_2 insult. *Invest. Ophthalmol. Vis. Sci.* **44**: 2084–2093. DOI: 10.1167/iovs.02-0882.

Halliwell B, Clement MV, Long LH. 2000. Hydrogen peroxide in the human body. *FEBS Lett.* **486**: 10–13. DOI: S0014-5793(00)02197-9.

Hamilton RF, Wu NQ, Porter D, Buford M, Wolfarth M, Holian A. 2009. Particle length-dependent titanium dioxide nanomaterials toxicity and bioactivity. *Part. Fibre Toxicol.* **6**. DOI: 10.1186/1743-8977-6-35.

Hanaor DAH, Sorrell CC. 2011. Review of the anatase to rutile phase transformation. *J. Mater. Sci.* **46**: 855–874.

Heng BC, Zhao X, Xiong S, Ng KW, Boey FY, Loo JS. 2010. Toxicity of zinc oxide (ZnO) nanoparticles on human bronchial epithelial cells (BEAS-2B) is accentuated by oxidative stress. *Food Chem. Toxicol.* **48**: 1762–1766. DOI: 10.1016/j.fct.2010.04.023.

Hoek JB, Pastorino JG. 2002. Ethanol, oxidative stress, and cytokine-induced liver cell injury. *Alcohol* **27**: 63–68. DOI: 10.1016/S0741-8329(02)00215-X.

Hu R, Gong X, Duan Y, Li N, Che Y, Cui Y, Zhou M, Liu C, Wang H, Hong F. 2010. Neurotoxicological effects and the impairment of spatial recognition memory in mice caused by exposure to TiO_2 nanoparticles. *Biomaterials* **31**: 8043–8050. DOI: 10.1016/j.biomaterials.2010.07.011.

Hunt JV, Dean RT, Wolff SP. 1988. Hydroxyl Radical Production and Autoxidative Glycosylation - Glucose Autoxidation as the Cause of Protein Damage in the Experimental Glycation Model of Diabetes-Mellitus and Aging. *Biochem. J.* **256**: 205–212.

Hussain S, Smulders S, De Vooght V, Ectors B, Boland S, Marano F, Van Landuyt KL, Nemery B, Hoet PH, Vanoirbeek JA. 2012. Nano-titanium dioxide modulates the dermal sensitization potency of DNCB. *Part. Fibre Toxicol.* **9**: 15. DOI: 10.1186/1743-8977-9-15.

Jenner P 2003. Oxidative stress in Parkinson's disease. *Ann. Neurol.* **53**: S26–S36. DOI: 10.1002/Ana.10483.

Jugan M-L, Barillet S, Simon-Deckers A, Herlin-Boime N, Sauvaigo S, Douki T, Carriere M. 2012. Titanium dioxide nanoparticles exhibit genotoxicity and impair DNA repair activity in A549 cells. *Nanotoxicology* **6**: 501–513. DOI: 10.3109/17435390.2011.587903.

Karasu C. 1999. Increased activity of H2O2 in aorta isolated from chronically streptozotocin-diabetic rats: effects of antioxidant enzymes and enzymes inhibitors. *Free Radic. Biol. Med.* **27**: 16–27.

Kim JA, Aberg C, Salvati A, Dawson KA. 2012. Role of cell cycle on the cellular uptake and dilution of nanoparticles in a cell population. *Nat. Nanotechnol.* **7**: 62–68. DOI: 10.1038/nnano.2011.191.

Kocbek P, Teskac K, Kreft ME, Kristl J. 2010. Toxicological aspects of long-term treatment of keratinocytes with ZnO and TiO_2 nanoparticles. *Small* **6**: 1908–1917. DOI: 10.1002/smll.201000032.

Kuo TR, Lee CF, Lin SJ, Dong CY, Chen CC, Tan HY. 2011. Studies of intracorneal distribution and cytotoxicity of quantum dots: risk assessment of eye exposure. *Chem. Res. Toxicol.* **24**: 253–261. DOI: 10.1021/tx100376n.

Lassoued S, Gargouri B, El Feki AF, Attia H, Van Pelt J. 2010. Transcription of the Epstein-Barr virus lytic cycle activator BZLF-1 during oxidative stress induction. *Biol. Trace Elem. Res.* **137**: 13–22. DOI: 10.1007/s12011-009-8555-y.

Li N, Ma LL, Wang J, Zheng L, Liu J, Duan YM, Liu HT, Zhao XY, Wang SS, Wang H, Hong F, Xie Y. 2010. Interaction between nano-anatase TiO_2 and liver DNA from mice *in vivo*. *Nanoscale Res. Lett.* **5**: 108–115. DOI: 10.1007/s11671-009-9451-2.

Liu HT, Ma LL, Zhao JF, Liu J, Yan JY, Ruan J, Hong FS. 2009. Biochemical toxicity of nano-anatase TiO2 particles in mice. *Biol. Trace Elem. Res.* **129**: 170–180. DOI: 10.1007/s12011-008-8285-6.

Loven D, Schedl H, Wilson H, Tahia T, Stegink LD, Diekus M, Oberly L. 1986. Effects of insulin and oral glutathione on glutathione levels and superoxide dismutase activities in organs of rats with streptozotocin-induced diabetes. *Diabetes* **35**: 503–507.

Magrez A, Horvath L, Smajda R, Salicio V, Pasquier N, Forro L, Schwaller B. 2009. Cellular toxicity of TiO_2-based nanofilaments. *ACS Nano* **3**: 2274–2280. DOI: 10.1021/nn9002067.

Maiorano G, Sabella S, Sorce B, Brunetti V, Malvindi MA, Cingolani R, Pompa PP. 2010. Effects of cell culture media on the dynamic formation of protein-nanoparticle complexes and influence on the cellular response. *ACS Nano* **4**: 7481–7491. DOI: 10.1021/nn101557e.

Malhi H, Gores GJ, Lemasters JJ. 2006. Apoptosis and necrosis in the liver: a tale of two deaths? *Hepatology* **43**: S31–44. DOI: 10.1002/hep.21062.

Mantena SK, King AL, Andringa KK, Eccleston HB, Bailey SM. 2008. Mitochondrial dysfunction and oxidative stress in the pathogenesis of alcohol- and obesity-induced fattyliver diseases. *Free Radic. Biol. Med.* **44**: 1259–1272. DOI: 10.1016/j.freeradbiomed.2007.12.029.

Marshall J. 2011. Draft Guidelines for Nanomedicine Unveiled. *Nature* doi:10.1038/news.2011.562.

Misawa M, Arai H. 1993. Airway inflammatory effect of hydrogen peroxide in guinea pigs. *J. Toxicol. Environ. Health* **38**: 435–448. DOI: 10.1080/15287399309531730.

Navarro CM, Montilla PM, Martin A, Jimenez J, Utrilla PM. 1993. Free radicals scavenger and antihepatotoxic activity of rosmarinus. *Plant Med.* **59**: 312–314. DOI: 10.1055/s-2006-959688.

Nojiri H, Shimizu T, Funakoshi M, Yamaguchi O, Zhou H, Kawakami S, Ohta Y, Sami M, Tachibana T, Ishikawa H, Kurosawa H, Kahn RC, Otsu K, Shirasawa T. 2006. Oxidative stress causes heart failure with impaired mitochondrial respiration. *J. Biol. Chem.* **281**: 33789–33801. DOI: 10.1074/jbc.M602118200.

Osuna O, Edds GT, Blankespoor HD. 1977. Toxic effects of aflatoxin B1 in male holstein calves with prior infection by Flukes (Fasciola hepatica). *Am. J. Vet. Res.* **38**: 341–349. DOI: oclc/50907294.

Qu Z, He X, Min L, Sha B, Shi X, Lu T, Xu F. 2013. Advances in the understanding of nanomaterial-biomembrane interactions and their mathematical and numerical modeling. *Nanomedicine* **8**: 1–17. DOI: 10.2217/NNM.13.81.

Ribeiro C, Vila C, M Elias de Matos J, Bettini J, Longo E, Leite ER. 2007. Role of the oriented attachment mechanism in the phase transformation of oxide nanocrystals. *Chemistry* **13**: 5798–5803. doi:10.1002/chem.200700034.

Roy S, Khanna S, Nallu K, Hunt TK, Sen CK. 2006. Dermal wound healing is subject to redox control. *Mol. Ther.* **13**: 211–220. DOI: 10.1016/j.ymthe.2005.07.684.

Rubin E, Lieber CS. 1974. Fatty liver, alcoholic hepatitis and cirrhosis produced by alcohol in primates. *New Engl. J. Med.* **290**: 128–135. DOI: 10.1056/NEJM197401172900303.

Sadauskas E, Danscher G, Stoltenberg M, Vogel U, Larsen A, Wallin H. 2009. Protracted elimination of gold nanoparticles from mouse liver. *Nanomedicine* **5**: 162–169. DOI: 10.1016/j.nano.2008.11.002.

Scaltriti M, Santamaria A, Paciucci R, Bettuzzi S. 2004. Intracellular clusterin induces G2-M phase arrest and cell death in PC-3 prostate cancer cells. *Cancer Res.* **64**: 6174–6182. DOI: 10.1158/0008-5472.CAN-04-0920.

Sciences M, Ene AC, Nwankwo EA, Samdi LM, Outstation M, Road GN. 2007. Alloxan-Induced Diabetes in Rats and the Effects of Black Caraway (Carum carvi L .) Oil on Their Body Weight. *J. Pharmacol. Toxicol.* **3**: 141–146. DOI: 10.3923/jpt.2008.141.146.

Sha B, Gao W, Wang S, Xu F, Lu T. 2011. Cytotoxicity of titanium dioxide nanoparticles differs in four liver cells from human and rat. *Compos. Part B-Eng.* **42**: 2136–2144. DOI: 10.1016/j.compositesb.2011.05.009.

Shackelford RE, Innes CL, Sieber SO, Heinloth AN, Leadon SA, Paules RS. 2001. The ataxia telangiectasia gene product is required for oxidative stress-induced G1 and G2 checkpoint function in human fibroblasts. *J. Biol. Chem.* **276**: 21951–21959. DOI: 10.1074/jbc.M011303200.

Shakoori AR, Butt U, Riffat R, Aziz F. 1994. Hematological and biochemical effects of danitol administered for two months on the blood and liver of rabbits. *Z. Angew. Zool.* **80**: 165–180.

Sha B, Gao W, Wang S, Liang X, Li W, Xu F, Lu T. 2013a. Nano-titanium dioxide increased cardiac injury in rat under oxidative stress. *Food Chem. Toxicol.* **58**: 280–288. DOI: 10.1016/j.fct.2013.04.050.

Sha B, Gao W, Han Y, Wang S, Wu J, Xu F, Lu T. 2013b. Potential application of titanium dioxide nanoparticles in the prevention of osteosarcoma and chondrosarcoma recurrence. *J. Nanosci. Nanotechnol.* **13**: 1208–1211. DOI: 10.1166/jnn.2013.6081.

Szkudelski T 2001. The mechanism of alloxan and streptozotocin action in B cells of the rat pancreas. *Physiol. Res.* **50**: 537–546.

Taurog A, Briggs FN, Chaikoff IL. 1952. I131-labeled 1-thyroxine. II. nature of the excretion product in bile. *J. Biol. Chem.* **194**: 655–668.

Thamaphat K, Limsuwan P, Ngotawornchai B. 2008. Phase Characterization of TiO2 Powder by XRD and TEM. *Technology* **361**: 357–361.

Tietz NW. 1976. *Fundamentals of Clinical Chemistry* (2nd ed.). WB Saunders Co: Philadelphia; 565–698.

Trouiller B, Reliene R, Westbrook A, Solaimani P, Schiestl RH. 2009. Titanium dioxide nanoparticles Induce DNA damage and genetic instability *in vivo* in mice. *Cancer Res.* **69**: 8784–8789. DOI: 10.1158/0008-5472.CAN-09-2496.

Umbreit TH, Francke-Carroll S, Weaver JL, Miller TJ, Goering PL, Sadrieh N, Stratmeyer ME. 2012. Tissue distribution and histopathological effects of titanium dioxide nanoparticles after intravenous or subcutaneous injection in mice. *J. Appl. Toxicol.* **32**: 350–357.

Van Gaal LF, Mertens IL, De Block CE. 2006. Mechanisms linking obesity with cardiovascular disease. *Nature* **444**: 875–880. DOI: 10.1038/nature05487.

Veronesi G, Brun E, Fayard B, Cotte M, Carriere M. 2012. Structural properties of rutile TiO_2 nanoparticles accumulated in a model of gastrointestinal epithelium elucidated by micro-beam x-ray absorption fine structure spectroscopy. *Appl. Phys. Lett.* **100**: 214101. DOI: 10.1063/1.4720172.

Vicent MJ, Duncan R. 2006. Polymer conjugates: nanosized medicines for treating Cancer. *Trends Biotechnol.* **24**: 39–47. DOI: 10.1016/j.tibtech.2005.11.006.

Vu HV, Acosta TJ, Yoshioka S, Abe H, Okuda K. 2012. Roles of prostaglandin F2alpha and hydrogen peroxide in the regulation of Copper/Zinc superoxide dismutase in bovine corpus luteum and luteal endothelial cells. *Reprod. Biol. Endocrinol.* **10**: 87. DOI: 10.1186/1477-7827-10-87.

Wang JX, Fan YB, Gao Y, Hu QH, Wang TC. 2009a. TiO2 nanoparticles translocation and potential toxicological effect in rats after intraarticular injection. *Biomaterials* **30**: 4590–4600. DOI: 10.1016/j.biomaterials.2009.05.008.

Wang F, Gao F, Lan M, Yuan H, Huang Y, Liu J. 2009b. Oxidative stress contributes to silica nanoparticle-induced cytotoxicity in human embryonic kidney cells. *Toxicol. Vitro* **23**: 808–815. DOI: 10.1016/j.tiv.2009.04.009.

Wang H, Xue Z, Wang Q, Feng X, Shen Z. 2008. Propofol protects hepatic L02 cells from hydrogen peroxide-induced apoptosis via activation of extracellular signal-regulated kinases pathway. *Anesth. Analg.* **107**: 534–540. DOI: 10.1213/ane.0b013e3181770be9.

Warheit DB, Brock WJ, Lee KP, Webb TR, Reed KL. 2005. Comparative pulmonary toxicity inhalation and instillation studies with different TiO_2 particle formulations:impact of surface treatments on particle toxicity. *Toxicol. Sci.* **88**: 514–524. DOI: 10.1093/toxsci/kfi331.

Warheit DB, Webb TR, Reed KL, Frerichs S, Sayes CM. 2007. Pulmonary toxicity study in rats with three forms of ultrafine-TiO2 particles: differential responses related to surface properties. *Toxicology* **230**: 90–104. DOI: 10.1016/j.tox.2006.11.002.

Wexler BC. 1981. Alloxan-induced diabetes in young vs old Sprague-Dawley rats. *Exp. Gerontol.* **16**: 47–58. DOI: 10.1016/0531-5565(81)90008-5

Wohaieb SA, Godin DV. 1987. Alterations in Free-Radical Tissue-Defense Mechanisms in Streptozocin-Induced Diabetes in Rat - Effects of Insulin-Treatment. *Diabetes* **36**: 1014–1018.

Yang SQ, Lin HZ, Lane MD, Clemens M, Diehl AM. 1997. Obesity increases sensitivity to endotoxin liver injury: implications for the pathogenesis of steatohepatitis. *Proc. Natl. Acad. Sci. U. S. A.* **94**: 2557–2562. DOI: 10.1073/pnas.94.6.2557.

Ye L, Yong KT, Liu L, Roy I, Hu R, Zhu J, Cai H, Law WC, Liu J, Wang K, Liu J, Liu Y, Hu Y, Zhang X, Swihart MT, Prasad PN. 2012. A pilot study in Non-human primates shows no adverse response to intravenous injection of quantum dots. *Nat. Nanotechnol.* **7**: 453–458. DOI: 10.1038/nnano.2012.74.

Zhang L, Bai R, Li B, Ge C, Du J, Liu Y, Le Guyader L, Zhao Y, Wu Y, He S, Ma Y, Chen C. 2011. Rutile TiO(2) particles exert size and surface coating dependent retention and lesions on the murine brain. *Toxicol. Lett.* **207**: 73–81. DOI: 10.1016/j.toxlet.2011.08.001.